A phenomenological model for the magneto-mechanical response of single-crystal Magnetic Shape Memory Alloys

Ferdinando Auricchio[a,c], Anne-Laure Bessoud[b], Alessandro Reali[a,c,*], Ulisse Stefanelli[c]

[a] *Dipartimento di Ingegneria Civile e Architettura, Università degli Studi di Pavia, via Ferrata 3, I-27100 Pavia, Italy*

[b] *Département BIOS, UMR AMAP, CIRAD, TA A-51 / PS2, Boulevard de la Lironde, F-34398 Montpellier Cedex 5, France*

[c] *Istituto di Matematica Applicata e Tecnologie Informatiche "Enrico Magenes" - CNR, via Ferrata 1, I-27100 Pavia, Italy*

Abstract

We advance a three-dimensional phenomenological model for the magneto-mechanical behavior of magnetic shape memory alloys. Moving from micromagnetic considerations, we propose a thermodynamically consistent constitutive relation which is able to reproduce the magnetically-induced martensitic transformation in single crystals. Existence results for the constitutive relation problem as well as for the corresponding quasi-static evolution system are illustrated and convergence of time- and space-time-discretizations are recorded. Eventually, we present algorithmic considerations and we numerically test the model in order to assess its ability in reproducing the typical response of magnetic shape-memory alloys.

Keywords: Magnetic Shape Memory Alloys, existence, discretization, numerical simulation.

1. Introduction

Shape-memory alloys (SMAs) are *active* materials: reversible strains as large as 10-12% can be induced by either thermal or mechanical stimuli [1]. This unique behavior is at the basis of a variety of innovative applications ranging from sensors and actuators, to Aerospace, Biomedical, and Seismic Engineering [2], just to mention a few hot application fields. Correspondingly, the interest for the efficient modeling, analysis, and control of SMAs behavior has triggered an intense research activity [3]. Without any claim of completeness, we shall refer to [4, 5, 6, 7, 8, 9, 10, 11, 12, 13, 14] for a collection of SMA modeling results.

Some SMAs (Ni$_2$MnGa, NiMnInCo, NiFeGaCo, FePt, FePd, among others) are called *magnetic* shape-memory alloys (MSMAs) as they feature a specific ferromagnetic behavior entailing a so-called *giant* magnetostrictive response. For instance, the 10% magnetostrictive strain of a

---

*Corresponding author.

Address: Dipartimento di Ingegneria Civile e Architettura, Università degli Studi di Pavia, via Ferrata 3, I-27100, Pavia, Italy

Phone/Fax: +39-0382-985704; E-mail: alessandro.reali@unipv.it

Ni$_2$MnGa single crystal (at a 1-3 MPa activation stress under the effect of a 1 T magnetic field) compares very favorably with the maximal 0.2% strain (at 60 MPa stress and 0.2 T field) in polycrystalline *TerFeNOL-D*, one of the highest performing magnetostrictive materials available to date.

The magnetic-induced strains in MSMAs are the macroscopic effect of the orientation of the ferromagnetic martensitic variants of the material. In particular, the martensitic phase in MSMAs presents the classical ferromagnetic texture of magnetic domains. This mesostructure changes under the influence of an external magnetic field by magnetic-domain wall motion, magnetization-vector rotation, and magnetic-field-driven martensitic-variant transformation. The first two effects above are present in all ferromagnetic materials. On the contrary, magnetic-field-driven variant transformation is a distinguishing trait of MSMAs. The interest in the possible applications of the unique material behavior of MSMAs is evident and may give some unprecedented possibility of activating devices (sensors, actuators, etc.) *at a distance* by specifically tuning an external magnetic field. Correspondingly, a vast Engineering literature is nowadays available on MSMAs. The reader shall be referred, with no claim of completeness, to [15, 16, 17, 18, 19, 20], see also the review in [21].

We introduce here a novel modeling of the magneto-mechanical response of MSMAs, already announced in [22, 23, 24]. Moving within the geometrically linear setting, we advance a three-dimensional, phenomenological, internal-variable-type description of MSMAs behavior which is able of replicate superelasticity, shape-memory, and magnetic shape-memory response as an effect of changes in magnetic field, stress, and absolute temperature. On the thermo-mechanical side, our model reproduces in the single-crystal setting the well-known *Souza-Auricchio* model for SMAs [25, 26, 27, 28], which has been proved to be very effective as well as extremely robust with respect to approximations. The Souza-Auricchio model has been analyzed from the viewpoint of existence and approximation of solutions in [29]. Moreover, it has been extended and analyzed in the connection with non-symmetric material behavior [30], residual plasticity [31, 32, 33], finite strains [34, 35, 36, 37, 38, 39], thermal evolution [40, 41] (given temperature) [42, 43, 44, 45] (unknown temperature), space discretizations [46, 47], and optimal control [48, 49].

Despite the effective tridimensionality of the model, we focus here on the assumption that martensites have a single *easy axis* of magnetization (i.e., we focus on the case of uniaxial magnetic materials). This is indeed the case for all known MSMAs which present either a cubic-to-tetragonal ($v = 3$ variants) or a cubic-to-orthorombic ($v = 6$ variants) systems (or, often a combination of both). Magnetic uniaxiality is deeply exploited in the modeling by choosing as internal variable the microscopic martensitic phase-fraction distribution $\boldsymbol{p} \in \mathbb{R}^v$ taking values in the simplex $S := \{p_i \geq 0, \ p_1 + \ldots + p_v \leq 1\}$. In particular, $\boldsymbol{p} = \boldsymbol{0}$ stands for a purely austenitic phase whereas $\boldsymbol{p}/(p_1 + \ldots + p_v)$ represents the local distribution of martensitic variants. Within this frame, we shall associate to each proportion $\boldsymbol{p}$ a specific *easy axis* $\boldsymbol{Ap}$ of magnetization, where $\boldsymbol{A}$ is a 3-tensor. Additionally, the *orientation* of the variants with respect to the easy axis will be determined by the scalar (signed) *magnetic-domain proportion* $\alpha \in [-1, 1]$.

The leading *ansatz* of our modeling is that the material presents a very strong magnetic anisotropy so that the actual magnetization of martensites is rigidly attached to the corresponding easy axes and no magnetization rotation actually takes place. In particular, given the phase distribution $\boldsymbol{p} \in S$, we require the magnetization $\boldsymbol{M}$ of the material to be given by

$$\boldsymbol{M} = m_{\mathrm{sat}} \alpha \boldsymbol{Ap} \tag{1.1}$$

2

where $m_{\text{sat}} > 0$ is the saturation magnetization. This assumption is in large agreement with observations on Ni_2MnGa [19, 20] in correspondence to the reference experimental (and applicative) situation. Still, the reader is referred to [50] for the mathematical analysis of a more general version of this model including magnetization rotations.

Before going on, let us briefly review some literature on MSMA modeling. Early modeling contributions have been mainly focusing on the energy minimization mechanism. Among these, we shall minimally refer to [15, 51, 52, 20, 53]. As for thermodynamically consistent models, one has to mention the contributions by [19, 54, 55]. A completely different perspective exploiting Preisach-type hysteretic relations is presented by [56]. An internal-variable model for MSMAs has been introduced by [57, 58] for two martensitic variants in two space dimensions. This model has then be extended to three variants by [59] where also the magnetic behavior of austenite is considered. Another internal-variable-type model has been proposed by [60, 61] again originally in the two-dimensional and two-variants setting (see also [62, 63]). This very model has been extended in order to encompass some more realistic magnetic response by [64]. A three-dimensional constitutive model with internal variables is proposed in [65], differing from ours mainly in the description of the magnetic state of the crystal. In particular, the magnetizations of single martensitic variants are there assumed to be collinear with the internal magnetic field whereas here magnetization is determined by p and no magnetization rotation is allowed. Finally, some micro-macro modeling perspective within the realm of irreversible thermodynamical processes is developed by [66, 67].

Apart from specific modeling choices, the striking distinctive trait of the present model with respect to the above mentioned propositions relies on its sound *variational structure* which in turn entails robustness with respect to approximations and discretizations. In particular, our model is presently the only one allowing a *full mathematical treatment* of the evolutive regime in terms of stability and convergence of time-incremental schemes, existence of solutions, and optimal controllability [24, 50]. Moreover, we have been able to establish rigorous Γ-convergence analyses [68] which in turn cross-validate the present model with respect to the original non-magnetic Souza-Auricchio model and to classical magnetoelasticity [24, 50]. An additional unique quality of our model is its remarkable simplicity: the knowledge of just 6 material parameters (concretely identifiable from experiments) is sufficient for the description of the full three-dimensional magnetomechanical behavior (see Subsection 2.4).

The paper is organized as follows. We devote Section 2 to the presentation of the model as well as to some discussion on its major features. The existence of *energetic solutions* [69], both at the constitutive equation and at the coupled quasi-static evolution level, are then recalled in Section 3. Algorithmic considerations as well as numerical simulations are reported in Section 4, while conclusions are drawn in Section 5. With respect to our previous contributions on this subject, the present paper brings a number of significant novelties. At the modeling level, we concentrate here on single MSMA crystals instead of polycrystals as the latter present reduced magnetostrictive effects and are hence less interesting for applications. A second novelty resides in the time-discretization scheme, here chosen to be semi-implicit, in consideration of the specific convex-concave structure of the reduced Gibbs energy, see Subsection 22.7. Finally, we present a novel convergence analysis of a full space-time-discrete scheme by a conformal finite element method.

2. The model

2.1. Tensor notation

In the following bold Latin letters stand for vectors in $\mathbb{R}^3$ and bold Greek symbols are for 2-tensors in $\mathbb{R}^3$. Given the 2-tensors $\boldsymbol{\alpha}$, $\boldsymbol{\beta} \in \mathbb{R}^{3 \times 3}$ and a 3-tensor $\boldsymbol{A} \in \mathbb{R}^{3 \times 3 \times 3}$, we classically define $\boldsymbol{\alpha}{:}\boldsymbol{\beta} \in \mathbb{R}$, $\boldsymbol{A}{:}\boldsymbol{\beta} \in \mathbb{R}^3$, and $\boldsymbol{\beta}{:}\boldsymbol{A} \in \mathbb{R}^3$ as (summation convention) $\boldsymbol{\alpha}{:}\boldsymbol{\beta} := \alpha_{ij}\beta_{ij}$, $(\boldsymbol{A}{:}\boldsymbol{\beta})_i := A_{ijk}\beta_{jk}$, $(\boldsymbol{\beta}{:}\boldsymbol{A})_k := \beta_{ij}A_{ijk}$, respectively. The space of symmetric 2-tensors is denoted by $\mathbb{R}^{3\times3}_{\mathrm{sym}}$ and endowed with the natural scalar product $\boldsymbol{\alpha}{:}\boldsymbol{\beta} := \mathrm{tr}(\boldsymbol{\alpha}\boldsymbol{\beta})$ where $\mathrm{tr}(\boldsymbol{\alpha}) := \alpha_{ii}$ and corresponding norm $|\boldsymbol{\alpha}|^2 := \boldsymbol{\alpha}{:}\boldsymbol{\alpha}$. Moreover, $\mathbb{R}^{3\times3}_{\mathrm{sym}}$ is orthogonally decomposed into $\mathbb{R}^{3\times3}_{\mathrm{sym}} = \mathbb{R}^{3\times3}_{\mathrm{dev}} \oplus \mathbb{R}\,\mathbf{1}_2$, where $\mathbb{R}\,\mathbf{1}_2$ is the subspace spanned by the identity 2-tensor $\mathbf{1}_2$ and $\mathbb{R}^{3\times3}_{\mathrm{dev}}$ is the subspace of deviatoric symmetric tensors. In particular, for all $\boldsymbol{\alpha} \in \mathbb{R}^{3\times3}_{\mathrm{sym}}$, we have that $\boldsymbol{\alpha} = \mathrm{dev}\,\boldsymbol{\alpha} + (\mathrm{tr}\,\boldsymbol{\alpha})\mathbf{1}_2/3$.

2.2. Mechanics

We recall here the modeling of thermo-mechanical (non-magnetic) SMA behavior from [25, 26, 27, 28] by adapting it to the specific situation of a single crystal. We describe the microscopic martensitic phase-fraction distribution of a MSMA single crystal by the vector $\boldsymbol{p} \in \mathbb{R}^v$ taking values in the simplex $S := \{p_i \geq 0,\ p_1 + \ldots + p_v \leq 1\}$. Recall that $\boldsymbol{p} = \mathbf{0}$ corresponds to austenite whereas $\boldsymbol{p} \in \{p_1 + \ldots + p_v = 1\}$ means pure martensite. We have specifically in mind the cases $v = 3$ and $v = 6$ which correspond to cubic-to-tetragonal (3 variants) cubic-to-orthorombic (6 variants) austenite-martensite systems. We shall use the symbols $\boldsymbol{p}^i \in \mathbb{R}^v$ to denote the canonical basis vectors in $\mathbb{R}^v$ or, equivalently, pure single martensitic phases.

Moving within the small-strain regime, we additively decompose the linearized deformation $\boldsymbol{\varepsilon}(\boldsymbol{u})$ given by $(\boldsymbol{\varepsilon}(\boldsymbol{u}))_{ij} := (u_{i,j} + u_{j,i})/2 \in \mathbb{R}^{3\times3}_{\mathrm{sym}}$ (here $\boldsymbol{u}$ denotes the displacement from the reference configuration) into the elastic part $\boldsymbol{\varepsilon}^{\mathrm{el}} \in \mathbb{R}^{3\times3}_{\mathrm{sym}}$ and the inelastic (or transformation) part $\boldsymbol{\varepsilon}_0(\boldsymbol{p}) \in \mathbb{R}^{3\times3}_{\mathrm{dev}}$ as

$$\boldsymbol{\varepsilon} = \boldsymbol{\varepsilon}^{\mathrm{el}} + \boldsymbol{\varepsilon}_0(\boldsymbol{p}). \tag{2.1}$$

In the latter, the linear map $\boldsymbol{p} \mapsto \boldsymbol{\varepsilon}_0(\boldsymbol{p}) \in \mathbb{R}^{3\times3}_{\mathrm{dev}}$ represents the deviatoric stress-free configuration corresponding to the phase distribution $\boldsymbol{p} = (p_1, \ldots, p_v)$. In particular,

$$\boldsymbol{\varepsilon}_0(\boldsymbol{p}) := \boldsymbol{\varepsilon}_0^i p_i \tag{2.2}$$

(summation convention) where $\boldsymbol{\varepsilon}_0^i := \boldsymbol{\varepsilon}_0(\boldsymbol{p}^i)$ is the stress-free reference configuration related to the i-th martensitic phase. In the cubic-to-tetragonal case ($v = 3$) we let

$$\boldsymbol{\varepsilon}_0^i := \frac{\varepsilon_L}{\sqrt{6}}\left(\mathbf{1}_2 - 3(\boldsymbol{e}^i \otimes \boldsymbol{e}^i)\right) \tag{2.3}$$

where $\boldsymbol{e}^i$ is the unit vector of the i-th axis in $\mathbb{R}^3$ and $\varepsilon_L > 0$ represents the maximal strain modulus obtainable via martensitic-variant transformation. Namely, we have

$$\boldsymbol{\varepsilon}_0^1 = \frac{\varepsilon_L}{\sqrt{6}}\begin{pmatrix} -2 & 0 & 0 \\ 0 & 1 & 0 \\ 0 & 0 & 1 \end{pmatrix}, \quad \boldsymbol{\varepsilon}_0^2 = \frac{\varepsilon_L}{\sqrt{6}}\begin{pmatrix} 1 & 0 & 0 \\ 0 & -2 & 0 \\ 0 & 0 & 1 \end{pmatrix}, \quad \boldsymbol{\varepsilon}_0^3 = \frac{\varepsilon_L}{\sqrt{6}}\begin{pmatrix} 1 & 0 & 0 \\ 0 & 1 & 0 \\ 0 & 0 & -2 \end{pmatrix} \tag{2.4}$$

As for the cubic-to-orthorombic case ($v = 6$), the stress-free strains are given by the six tensors

$$\boldsymbol{\varepsilon}_0^i := \frac{\varepsilon_L}{c_\gamma}\Big((1+\gamma)(\mathbf{1}_2 - 3(\boldsymbol{e}^i \otimes \boldsymbol{e}^i)) \pm (1-\gamma)(\boldsymbol{e}^j \otimes \boldsymbol{e}^k + \boldsymbol{e}^k \otimes \boldsymbol{e}^j)\Big)$$

for $i, j, k \in \{1, 2, 3\}$ distinct, $\gamma > 0$ being a specific alloy-dependent crystallographic parameter. In particular, we have

$$\boldsymbol{\varepsilon}_0^1 = \frac{\varepsilon_L}{c_\gamma} \begin{pmatrix} -2-2\gamma & 0 & 0 \\ 0 & 1+\gamma & 1-\gamma \\ 0 & 1-\gamma & 1+\gamma \end{pmatrix}, \quad \boldsymbol{\varepsilon}_0^2 = \frac{\varepsilon_L}{c_\gamma} \begin{pmatrix} -2-2\gamma & 0 & 0 \\ 0 & 1+\gamma & \gamma-1 \\ 0 & \gamma-1 & 1+\gamma \end{pmatrix}$$

$$\boldsymbol{\varepsilon}_0^3 = \frac{\varepsilon_L}{c_\gamma} \begin{pmatrix} 1+\gamma & 0 & 1-\gamma \\ 0 & -2-2\gamma & 0 \\ 1-\gamma & 0 & 1+\gamma \end{pmatrix}, \quad \boldsymbol{\varepsilon}_0^4 = \frac{\varepsilon_L}{c_\gamma} \begin{pmatrix} 1+\gamma & 0 & \gamma-1 \\ 0 & -2-2\gamma & 0 \\ \gamma-1 & 0 & 1+\gamma \end{pmatrix},$$

$$\boldsymbol{\varepsilon}_0^5 = \frac{\varepsilon_L}{c_\gamma} \begin{pmatrix} 1+\gamma & 1-\gamma & 0 \\ 1-\gamma & 1+\gamma & 0 \\ 0 & 0 & -2-2\gamma \end{pmatrix}, \quad \boldsymbol{\varepsilon}_0^6 = \frac{\varepsilon_L}{c_\gamma} \begin{pmatrix} 1+\gamma & \gamma-1 & 0 \\ \gamma-1 & 1+\gamma & 0 \\ 0 & 0 & -2-2\gamma \end{pmatrix},$$

where $c_\gamma = \sqrt{8(1+\gamma+\gamma^2)}$ is a normalization constant entailing $|\boldsymbol{\varepsilon}_0^i| = \varepsilon_L$.

2.3. Magnetics

We assume each martensitic variant to show a single *easy axis* of magnetization. In particular, we assume that the linear relation $\boldsymbol{p} \mapsto \boldsymbol{A}\boldsymbol{p}$ for some given $\boldsymbol{A} \in \mathbb{R}^{3 \times v}$ gives the (directed) easy axis of the phase distribution $\boldsymbol{p}$. Our choice for $\boldsymbol{A}$ is

$$\boldsymbol{A} := \mathbf{1}_2 \quad \text{for } v = 3, \qquad \boldsymbol{A} := \begin{pmatrix} 1 & 1 & 0 & 0 & 0 & 0 \\ 0 & 0 & 1 & 1 & 0 & 0 \\ 0 & 0 & 0 & 0 & 1 & 1 \end{pmatrix}^\top \qquad \text{for } v = 6.$$

Additionally, the *orientation* of the variants with respect to the easy axis will be determined by the scalar $\alpha \in [-1, 1]$ which is then to be interpreted as the *magnetic-domain (signed) proportion*.

Our theory will rely on the *strong magnetic-anisotropy ansatz* (1.1). In particular, note that position (1.1) entails that the austenitic phase is non-magnetic. This is indeed a simplification as austenite in MSMAs shows generically a cubic-anisotropic magnetic behavior. On the other hand, this simplification is motivated by the fact that the austenitic magnetic character is generally not exploited in applications. Coherently, our numerical tests are performed at some suitably low temperature, so that the possible magnetic behavior of austenite does not play any role.

One has to mention that all MSMA models proposed so far deal specifically with MSMAs single crystals. We shall indeed remark that MSMAs polycrystals, despite their relatively easier production process, have attracted much less attention and, in particular, are presently not yet exploited in real devices. This is motivated by the observed significant drop in the observed

5

magnetostrictive strain in polycrystals vs. single crystals [70]. This drop is probably the outcome of the relatively poor martensitic-variant structure of all MSMAs to date (tetragonal, orthorombic) and is triggered by the strong kinematic and magnetic compatibility constraints at grain boundaries. Moreover, one shall observe that the MSMA polycrystals available to date are extremely brittle [71].

2.4. Gibbs energy

The constitutive relations for the model are derived from the specification of the Gibbs free energy density of the material (which we assume to be of a constant and normalized density) as a function of the stress $\boldsymbol{\sigma}$, the internal magnetic field $\boldsymbol{H}$, the absolute temperature T, and the internal variables $\boldsymbol{p}$ and α as

$$G(\boldsymbol{\sigma}, \boldsymbol{H}, T, \boldsymbol{p}, \alpha) := -\frac{1}{2}\boldsymbol{\sigma}{:}\mathbb{C}^{-1}{:}\boldsymbol{\sigma} - \boldsymbol{\sigma}{:}\boldsymbol{\varepsilon}_0(\boldsymbol{p}) + \beta(T)|\boldsymbol{\varepsilon}_0(\boldsymbol{p})| + \frac{h}{2}|\boldsymbol{\varepsilon}_0(\boldsymbol{p})|^2 + I_S(\boldsymbol{p})$$

$$+ \frac{1}{2\delta}\alpha^2 + I_{[-1,1]}(\alpha) - \mu_0 \boldsymbol{H}{\cdot}m_{\text{sat}}\alpha \boldsymbol{A}\boldsymbol{p}. \tag{2.5}$$

The first line in (2.5) is exactly the Gibbs energy of the Souza-Auricchio model for non-magnetic SMAs [25, 28]. In particular $\mathbb{C}$ is the isotropic elasticity 4-tensor, fulfilling indeed classical symmetries $\mathbb{C}_{ij\ell k} = \mathbb{C}_{ji\ell k} = \mathbb{C}_{\ell k ij}$, $T \mapsto \beta(T) \geq 0$ is a given function of the temperature which represents the temperature-dependence of the activation stress for the martensite-austenite phase transformation, $h > 0$ is the kinematic hardening modulus (here assumed to be isotropic), and I_S is the *indicator function* of the simplex S (namely $I_S(\boldsymbol{p}) = 0$ if $\boldsymbol{p} \in S$ and $I_S(\boldsymbol{p}) = \infty$ otherwise).

As temperature effects are not of interest here, we fix right from the beginning some suitable temperature T^* (under the Curie temperature) such that field-induced transformation of martensitic variants may take place. Correspondingly, β^* stands for the constant nonnegative value $\beta(T^*)$.

In the following, we shall use the short-hand notation

$$F_{\text{SA}}(\boldsymbol{p}) := \beta^*|\boldsymbol{\varepsilon}_0(\boldsymbol{p})| + \frac{h}{2}|\boldsymbol{\varepsilon}_0(\boldsymbol{p})|^2 + I_S(\boldsymbol{p}),$$

in order to indicate the specific choice of the original Souza-Auricchio model for the mechanical hardening part of the Gibbs energy.

The second line in the expression of the Gibbs energy (2.5) describes the magnetic behavior of the material. The term $-\mu_0 \boldsymbol{H}{\cdot}m_{\text{sat}}\alpha \boldsymbol{A}\boldsymbol{p}$ is nothing but the classical *Zeeman energy* term $-\mu_0 \boldsymbol{H}{\cdot}\boldsymbol{M}$. Note that $\boldsymbol{H}$ stands here for the *internal* magnetic field. Namely, $\boldsymbol{H}$ is the magnetic field which is actually experienced by the material when subjected to some (externally) applied field. In particular, $\boldsymbol{H}$ corresponds to the sum of the applied external field and the corresponding induced demagnetization field. We will proceed by assuming that the field $\boldsymbol{H}$ is known for all times. This is indeed a simplification as the induced demagnetization field, thus $\boldsymbol{H}$, depends on the deformation state of the specimen via Maxwell's system. By neglecting this coupling we are indeed concentrating on situations where the demagetization field is of lower order with respect to the external field. This is particularly the case for thin Ni_2MnGa body with respect to the correspondingly high activation fields.

The indicator function $I_{[-1,1]}$ constraints the signed domain proportion α to take values in $[-1,1]$ and $1/\delta$ is a user-defined (dimensionalized in MPa) hardening-like parameter modulating the tendency of magnetic domains to equilibrated configurations $\alpha = 0$.

2.5. Constitutive equations

Given the Gibbs energy (2.5), we classically derive the constitutive equations by letting

$$\boldsymbol{\varepsilon} \quad = -\frac{\partial G}{\partial \boldsymbol{\sigma}} = \mathbb{C}^{-1}{:}\boldsymbol{\sigma} + \boldsymbol{\varepsilon}_0(\boldsymbol{p}), \tag{2.6}$$

$$\boldsymbol{M} \quad = -\frac{1}{\mu_0}\frac{\partial G}{\partial \boldsymbol{H}} = m_{\text{sat}}\alpha\boldsymbol{A}\boldsymbol{p}, \tag{2.7}$$

$$\boldsymbol{\xi} \quad \in -\frac{\partial G}{\partial \boldsymbol{p}} = \boldsymbol{\sigma}{:}\partial_{\boldsymbol{p}}\boldsymbol{\varepsilon}_0(\boldsymbol{p}) - \beta^*\partial_{\boldsymbol{p}}|\boldsymbol{\varepsilon}_0(\boldsymbol{p})| - h\boldsymbol{\varepsilon}_0(\boldsymbol{p}){:}\partial_{\boldsymbol{p}}\boldsymbol{\varepsilon}_0(\boldsymbol{p}) - \partial_{\boldsymbol{p}}I_S(\boldsymbol{p}) + \mu_0 m_{\text{sat}}\alpha\boldsymbol{H}\boldsymbol{A}, \tag{2.8}$$

$$g \quad \in -\frac{\partial G}{\partial \alpha} = -\frac{1}{\delta}\alpha - \partial I_{[-1,1]}(\alpha) + \mu_0 m_{\text{sat}}\boldsymbol{H}{\cdot}\boldsymbol{A}\boldsymbol{p}. \tag{2.9}$$

Here, $\boldsymbol{\xi} \in \mathbb{R}^v$ and $g \in \mathbb{R}$ are the *thermodynamic forces* associated with the internal variables $\boldsymbol{p}$ and α, respectively. The symbol ∂ denotes the subdifferential in the sense of Convex Analysis [72]. In particular, we have that $(\partial_{\boldsymbol{p}}\boldsymbol{\varepsilon}_0(\boldsymbol{p}))_{ijk} = (\boldsymbol{\varepsilon}_0^k)_{ij}$ and we define, for brevity $\boldsymbol{E} := \partial_{\boldsymbol{p}}\boldsymbol{\varepsilon}_0(\boldsymbol{p})$. Moreover,

$$\boldsymbol{\beta} \in \partial_{\boldsymbol{p}}|\boldsymbol{\varepsilon}_0(\boldsymbol{p})| \quad \Longleftrightarrow \quad \boldsymbol{\beta}{:}(\boldsymbol{q}-\boldsymbol{p}) \le |\boldsymbol{\varepsilon}_0(\boldsymbol{q})| - |\boldsymbol{\varepsilon}_0(\boldsymbol{p})| \quad \forall \boldsymbol{q} \in \mathbb{R}^v$$

which entails that

$$(\partial_{\boldsymbol{p}}|\boldsymbol{\varepsilon}_0(\boldsymbol{p})|)_k = \frac{\boldsymbol{\varepsilon}_0(\boldsymbol{p}){:}\boldsymbol{\varepsilon}_0^k}{|\boldsymbol{\varepsilon}_0(\boldsymbol{p})|} = \frac{\boldsymbol{\varepsilon}_0(\boldsymbol{p}){:}\boldsymbol{E}}{|\boldsymbol{\varepsilon}_0(\boldsymbol{p})|} \quad \text{for all} \quad \boldsymbol{\varepsilon}_0(\boldsymbol{p}) \ne \boldsymbol{0}.$$

2.6. Flow rule

We shall assume that the phase transformation dissipates energy (exactly as in the original non-magnetic Souza-Auricchio model) whereas the evolution of the magnetic-domain proportion α is non-dissipative. This is of course disputable as the dissipation in α is, indeed, the basic dissipative mechanism in ferromagnetic materials. Still, MSMA experiments show that, at small strains, the dissipation in α is negligible with respect to that in $\boldsymbol{p}$ [73, 60]. Plus, we shall comment that including the dissipative character of α in the model would be straightforward (and, to some extent, even better from the mathematical view point).

The evolution of the material is prescribed via a normality assumption. In particular, we prescribe the yield function $F : \mathbb{R}^v \to \mathbb{R}$

$$F(\boldsymbol{\xi}) := |\boldsymbol{\xi}| - R$$

where $R > 0$ is the activation radius, and require $\dot{\boldsymbol{p}}$ to satisfy the classical complementary conditions

$$\dot{\boldsymbol{p}} = \dot{\zeta}\partial F(\boldsymbol{\xi}), \quad \dot{\zeta} \ge 0, \quad F \le 0, \quad \dot{\zeta}F = 0.$$

The latter can be reformulated in a more compact form by means of the dissipation function $D(\dot{\boldsymbol{p}}) := R|\dot{\boldsymbol{p}}|$ as the inclusion

$$\boldsymbol{\xi} \in \partial D(\dot{\boldsymbol{p}}). \tag{2.10}$$

2.7. Reduced formulation

As the magnetic-domain proportion α is non-dissipative, we have that the thermodynamic force g vanishes. Hence, by solving relation (2.9) for $g = 0$ one can obtain α as a function of $\boldsymbol{H}$ and $\boldsymbol{p}$. In particular, we have that

$$\alpha = \Pi_{[-1,1]}\big(\delta\mu_0 m_{\mathrm{sat}}\boldsymbol{H}\cdot\boldsymbol{Ap}\big) := \max\big\{-1, \min\big\{1, \delta\mu_0 m_{\mathrm{sat}}\boldsymbol{H}\cdot\boldsymbol{Ap}\big\}\big\} \tag{2.11}$$

where $\Pi_{[-1,1]}$ denotes the projection onto $[-1,1]$. In other words, one can minimize out α from the Gibbs energy (2.5) in order to obtain a *reduced* formulation. The minimum is attained exactly at $\alpha = \Pi_{[-1,1]}\big(\delta\mu_0 m_{\mathrm{sat}}\boldsymbol{H}\cdot\boldsymbol{Ap}\big)$ so that

$$
\begin{aligned}
G_{\mathrm{red}}(\boldsymbol{\sigma}, \boldsymbol{H}, T, \boldsymbol{p}) \quad &:= \quad \min_{\alpha} G(\boldsymbol{\sigma}, \boldsymbol{H}, T, \boldsymbol{p}, \alpha) \\
&= \quad -\frac{1}{2}\boldsymbol{\sigma}{:}\mathbb{C}^{-1}{:}\boldsymbol{\sigma} - \boldsymbol{\sigma}{:}\varepsilon_0(\boldsymbol{p}) + F_{\mathrm{SA}}(\boldsymbol{p}) \\
&+ \quad \frac{1}{2\delta}\big(\Pi_{[-1,1]}\big(\delta\mu_0 m_{\mathrm{sat}}\boldsymbol{H}\cdot\boldsymbol{Ap}\big)\big)^2 - \mu_0 m_{\mathrm{sat}}\Pi_{[-1,1]}\big(\delta\mu_0 m_{\mathrm{sat}}\boldsymbol{H}\cdot\boldsymbol{Ap}\big)\boldsymbol{H}\boldsymbol{Ap} \\
&= \quad -\frac{1}{2}\boldsymbol{\sigma}{:}\mathbb{C}^{-1}{:}\boldsymbol{\sigma} - \boldsymbol{\sigma}{:}\varepsilon_0(\boldsymbol{p}) + F_{\mathrm{SA}}(\boldsymbol{p}) - F_{\mathrm{mag}}(\boldsymbol{H}\cdot\boldsymbol{Ap}).
\end{aligned}
$$

In the latter we have introduced the convex function $F_{\mathrm{mag}} \in C^{1,1}(\mathbb{R})$ given by

$$F_{\mathrm{mag}}(r) := \frac{1}{2\delta}\min\big\{(\delta\mu_0 m_{\mathrm{sat}}r)^2, 2|\delta\mu_0 m_{\mathrm{sat}}r| - 1\big\} \quad \text{for all } r \in \mathbb{R}.$$

In particular, we have that $F'_{\mathrm{mag}}(r) = \mu_0 m_{\mathrm{sat}}\Pi_{[-1,1]}(\delta\mu_0 m_{\mathrm{sat}}r)$ so that

$$\mathrm{D}_{\boldsymbol{p}}F_{\mathrm{mag}}(\boldsymbol{H}\cdot\boldsymbol{Ap}) = \mu_0 m_{\mathrm{sat}}\Pi_{[-1,1]}(\delta\mu_0\boldsymbol{H}\cdot\boldsymbol{Ap})\boldsymbol{HA} = \mu_0 m_{\mathrm{sat}}\alpha\boldsymbol{HA}$$

and we can rewrite the last term in the right-hand side of relation (2.8) as $\mathrm{D}_{\boldsymbol{p}}F_{\mathrm{mag}}(\boldsymbol{H}\cdot\boldsymbol{Ap})$.

2.8. Constitutive relation

Given the above arguments, the final form of the constitutive equation problem reads

$$\partial D(\dot{\boldsymbol{p}}) + \partial F_{\mathrm{SA}}(\boldsymbol{p}) - \mathrm{D}_{\boldsymbol{p}}F_{\mathrm{mag}}(\boldsymbol{H}\cdot\boldsymbol{Ap}) \ni \boldsymbol{\sigma}{:}\boldsymbol{E} \tag{2.12}$$

where we recall that $\boldsymbol{E} = \partial_{\boldsymbol{p}}\varepsilon_0(\boldsymbol{p})$ is independent of $\boldsymbol{p}$. Moreover, note that we have $\boldsymbol{\sigma}{:}\boldsymbol{E} = \mathrm{dev}\,\boldsymbol{\sigma}{:}\boldsymbol{E}$. In particular, the evolution of $\boldsymbol{p}$ is driven by the deviator $\mathrm{dev}\,\boldsymbol{\sigma}$ only.

2.9. Mechanical and magnetic saturation

Given position (2.2), one readily checks the mechanical saturation constraint

$$|\varepsilon_0(\boldsymbol{p})| = \left|\sum_{i=1}^{v}p_i\varepsilon_0^i\right| \le \sum_{i=1}^{v}p_i|\varepsilon_0^i| = \varepsilon_L(p_1 + \cdots + p_v) \le \varepsilon_L$$

is fulfilled by all phases $\boldsymbol{p} \in S$. In particular, mechanical saturation $|\varepsilon_0(\boldsymbol{p})| = \varepsilon_L$ occurs if and only if $\boldsymbol{p}$ corresponds to a pure single martensitic phase, i.e., $\boldsymbol{p} = \boldsymbol{p}^i$ for some $i = 1, \ldots, v$.

As for the magnetic saturation, from (1.1) we have that

$$|\boldsymbol{M}| = |m_{\mathrm{sat}}\alpha\boldsymbol{Ap}| \le m_{\mathrm{sat}}|\alpha|\,|\boldsymbol{Ap}| \le m_{\mathrm{sat}}.$$

Note that $|\boldsymbol{Ap}| \le 1$ for $\boldsymbol{p} \in S$ for both $v = 3$ and $v = 6$. Again, magnetic saturation occurs just in connection with pure, single, and completely oriented ($\alpha \equiv 1$ or $\alpha \equiv -1$) phases.

8

2.10. Kinematic and magnetic compatibility

In both cases $v = 3$ and $v = 6$ martensitic variants are pairwise kinematically [74] and magnetically compatible [15]. In particular, given any pair of pure phases $\boldsymbol{p}^i$, $\boldsymbol{p}^j$ there exist $\boldsymbol{a}^{ij}$, $\boldsymbol{n}^{ij} \in \mathbb{R}^3$ such that

$$\boldsymbol{\varepsilon}_0(\boldsymbol{p}^i) - \boldsymbol{\varepsilon}_0(\boldsymbol{p}^j) = \frac{1}{2}\Big(\boldsymbol{a}^{ij}{\otimes}\boldsymbol{n}^{ij} + \boldsymbol{n}^{ij}{\otimes}\boldsymbol{a}^{ij}\Big), \tag{2.13}$$

$$\boldsymbol{A}\boldsymbol{p}^i - \boldsymbol{A}\boldsymbol{p}^j = \boldsymbol{n}^{ij}. \tag{2.14}$$

Condition (2.13) ensures that there exists a nontrivial continuous deformation such that $\boldsymbol{\varepsilon}(\boldsymbol{u})$ takes value in $\{\boldsymbol{\varepsilon}_0^i, \boldsymbol{\varepsilon}_0^j\}$ across the discontinuity surface for the strain. In particular, $\boldsymbol{a}^{ij}$, $\boldsymbol{n}^{ij}$ are the two possible normals to such surface. On the other hand, condition (2.14) asserts that the interfaces with normal $\boldsymbol{n}^{ij}$ serve as pole-free surfaces of discontinuity of the magnetization. The check of (2.13)-(2.14) is immediate in the cubic-to-tetragonal case $v = 3$ [74] and requires some tedious algebraic elaboration in the cubic-to-orthorombic case $v = 6$.

From the purely mechanical viewpoint one has however to observe that the proposed model does not include the description of compatibility constraints between martensitic variants and austenite. In other words, the assumption $\boldsymbol{p} \in S$ is indeed a simplification as some phase proportions in the region $\{p_1 + \ldots + p_v < 1\}$ may be not accessible to real materials due to (the lack of) kinematic compatibility. We shall however stick to the latter simplification as it does not jeopardize the outcome of the model and allows for a rather complete mathematical treatment.

2.11. Blocking stress and Nucleation vs Magnetization rotation

The ferromagnetic behavior of the material is highly stress-dependent [17, 54]. When applying a compressive stress in direction $(1, 0, 0)$, above some fixed (and rather small) *blocking stress* level no variant transformation can be induced by magnetic fields of the form $\boldsymbol{H} = (0, H_2, H_3)$.

This effect is predicted by our model, although to some schematic extent. Indeed, as soon as the compressive stress is such that martensite is fully oriented into variant $\boldsymbol{p}^1$ for $v = 3$ (or $\boldsymbol{p}^1$ and $\boldsymbol{p}^2$ for $v = 6$), the corresponding magnetic-domain proportion is

$$\alpha = \Pi_{[-1,1]}(\delta\mu_0 m_{\text{sat}}\boldsymbol{H}{\cdot}\boldsymbol{e}^1) = \Pi_{[-1,1]}(\delta\mu_0 m_{\text{sat}}H_1) = 0.$$

Hence, the magneto-mechanical coupling term vanishes and no magnetically-induced variant transformation occurs. On the other hand, independently of the stress level, in case $\boldsymbol{p} \neq \boldsymbol{p}^1$ (or $\boldsymbol{p} \neq \boldsymbol{p}^1$, $\boldsymbol{p}^2$ for $v = 6$) the model predicts variant transformation by $\boldsymbol{H} = (0, H_2, H_3)$. Finally, even in the saturated case $\boldsymbol{p} = \boldsymbol{p}^1$ ($\boldsymbol{p} \neq \boldsymbol{p}^1$, $\boldsymbol{p}^2$ for $v = 6$), one can induce variant transformation by letting $H_1 \neq 0$. This behavior agrees with observations and with the strong anisotropy assumption from (1.1). Indeed, experimental evidences suggest that the applied field moves primarily variant interfaces that are already present. Starting from a pure-variant martensitic state, nucleation of another variant occurs at some relatively high energy expense and magnetization rotation is preferred [53]. Our model reflects this phenomenon by preventing transformation of pure phases under specific magnetic fields.

3. Existence and approximation of solutions

As mentioned above, a remarkable trait of the present model is its variational structure which make it amenable to an efficient mathematical treatment. In particular, global existence results for solutions to the constitutive relation and to the quasi-static evolution problem has well as the convergence of implicit time-discretizations have been obtained in [24]. We shall recall these results here and complement them in the direction of fully discrete schemes.

3.1. Constitutive relation problem

Given the stress $t \in [0,T] \mapsto \boldsymbol{\sigma}(t) \in \mathbb{R}^{3\times 3}_{\text{sym}}$, the internal magnetic field $t \mapsto \boldsymbol{H}(t) \in \mathbb{R}^3$, and the initial state $\boldsymbol{p}^0 \in \mathbb{R}^v$ we are interested in finding a *variational* solution of the constitutive relation (2.12). In particular, we shall exploit the notion of *energetic solution* (of the constitutive relation) introduced by in [75]. By defining the *total energy*

$$E(t, \boldsymbol{p}) := F_{\text{SA}}(\boldsymbol{p}) - F_{\text{mag}}(\boldsymbol{H}(t){\cdot}\boldsymbol{Ap}) - \boldsymbol{\sigma}(t){:}\boldsymbol{E},$$

we search for a trajectory $t \in [0,T] \mapsto \boldsymbol{p}(t) \in \mathbb{R}^v$ with $\boldsymbol{p}(0) = \boldsymbol{p}^0$ fulfilling $F'_{\text{mag}}(\boldsymbol{H}{\cdot}\boldsymbol{Ap})\dot{\boldsymbol{H}}{\cdot}\boldsymbol{Ap} \in L^1(0,T)$, and, for all $t \in [0,T]$,

Stability:
$$E(t, \boldsymbol{p}(t)) < \infty \quad \text{and} \quad E(t, \boldsymbol{p}(t)) \le E(t, \widehat{\boldsymbol{p}}) + D(\widehat{\boldsymbol{p}}{-}\boldsymbol{p}(t)) \quad \forall \widehat{\boldsymbol{p}} \in S; \tag{3.1}$$

Energy balance:
$$E(t, \boldsymbol{p}(t)) + \text{Diss}(\boldsymbol{p}, [0,t]) \le E(0, \boldsymbol{p}^0) - \int_0^t \dot{\boldsymbol{\sigma}}{:}\boldsymbol{E} - \int_0^t F'_{\text{mag}}(\boldsymbol{H}{\cdot}\boldsymbol{Ap})\dot{\boldsymbol{H}}{\cdot}\boldsymbol{Ap}. \tag{3.2}$$

Relation (3.1) encodes the so-called *global stability*: by comparing the energy of the actual state $\boldsymbol{p}(t)$ with that of a competitor state $\widehat{\boldsymbol{p}}$, the energy difference is $E(t, \widehat{\boldsymbol{p}}) - E(t, \boldsymbol{p}(t))$ is smaller or equal to the dissipation distance is $D(\widehat{\boldsymbol{p}}{-}\boldsymbol{p}(t))$. We say that a state $\boldsymbol{p}(t)$ is *stable* at time t if it fulfills (3.1).

On the other hand, relation (3.2) represents energy conservation. In particular, the term

$$\text{Diss}(\boldsymbol{p}, [0,t]) := \sup\left\{ \sum_{i=1}^n D(\boldsymbol{p}(t_i){-}\boldsymbol{p}(t_{i-1})) \, : \, 0{=}t_0{<}t_1{<}\ldots{<}t_n{=}t \right\}, \tag{3.3}$$

(the sup being taken among all partitions of $[0,t]$) represents the dissipated energy along the interval $[0,t]$. Finally, the integral terms in the right-hand side of (3.2) stand for the work done by the external actions. We have the following existence result.

Theorem 3.1 (Existence for the constitutive relation (Thm. 3.1 [24]))**.** *Let* $\boldsymbol{\sigma} \in W^{1,1}(0,T; \mathbb{R}^{3\times 3}_{\text{sym}})$, $\boldsymbol{H} \in W^{1,1}(0,T; \mathbb{R}^3)$, *and* $\boldsymbol{p}^0 \in \mathbb{R}^v$ *be stable at* $t = 0$. *Then, there exists an energetic solution of the constitutive relation.*

Let us mention that the proof of the above existence result is constructive for an energetic solution can be obtained by passing to the limit in a sequence of time-discrete problems. In particular, by letting $\{0=t_m^0<t_m^1<\ldots<t_m^{N_m}=T\}$, $m \in \mathbb{N}$, be a sequence of partitions of $[0,T]$ with diameters $\tau_m := \max_i(t_m^i-t_m^{i-1}) \to 0$ for $m \to \infty$, one fixes $\boldsymbol{p}_m^0 = \boldsymbol{p}_0$ and considers the incremental minimization problems

$$\boldsymbol{p}_m^k \in \arg\min\left(E(t_m^k,\boldsymbol{p}) + D(\boldsymbol{p}-\boldsymbol{p}_m^{k-1})\right) \quad \text{for} \quad k=1,\ldots,N_m. \tag{3.4}$$

This sequence of minimization problems possesses a solution due to the fact that the functionals to be minimized are coercive and lower semicontinuous. In particular, as the nonconvex term F_{mag} is smooth, we can equivalently reformulate the minimization problem (3.4) as that of finding $\boldsymbol{p}_m^k$ solving the implicit Euler scheme

$$\partial D(\boldsymbol{p}_m^k-\boldsymbol{p}_m^{k-1}) + \partial F_{\text{SA}}(\boldsymbol{p}_m^k) - \mathrm{D}_{\boldsymbol{p}}F_{\text{mag}}(\boldsymbol{H}(t_m^k)\cdot\boldsymbol{A}\boldsymbol{p}_m^k) \ni \boldsymbol{\sigma}(t_m^k){:}\boldsymbol{E} \quad \text{for} \quad k=1,\ldots,N_m. \tag{3.5}$$

Given the discrete-solution vector $\{\boldsymbol{p}_m^k\}_{k=0}^{N_m}$, let us denote by $\boldsymbol{p}_m$ the corresponding right-continuous piecewise constant interpolant on the time-partition. We have the following convergence result.

Theorem 3.2 (Convergence of time-discretizations (Cor. 3.1 [24])). *Up to not relabeled subsequences we have that, for all $t \in [0,T]$,*

$$\boldsymbol{p}_m(t) \to \boldsymbol{p}(t), \quad E(t,\boldsymbol{p}_m(t)) \to E(t,\boldsymbol{p}(t)), \quad \text{Diss}(\boldsymbol{p}_m,[0,t]) \to \text{Diss}(\boldsymbol{p},[0,t])$$

where $\boldsymbol{p}$ is an energetic solution of the constitutive relation.

3.2. Semi-implicit scheme

The fully implicit scheme from (3.5) is particularly suited for proving existence of energetic solutions. On the other hand, it performs somehow poorly in connection with comparably large time steps (i.e., large changes in data), especially starting from some non-magnetized situation ($\alpha = 0$). This is due to the local concavity of $E(t,\cdot)$ around the zero-magnetization state (note however that $E(t,\cdot)$ is convex and coercive far from it). In particular, due to non-convexity the discrete incremental problem may admit multiple solutions. A possible way to circumvent this difficulty is that of considering a semi-implicit scheme in which the magnetization part of the energy is evaluated explicitly, namely

$$\partial D(\boldsymbol{p}_m^k-\boldsymbol{p}_m^{k-1}) + \partial F_{\text{SA}}(\boldsymbol{p}_m^k) - \mathrm{D}_{\boldsymbol{p}}F_{\text{mag}}(\boldsymbol{H}(t_m^k)\cdot\boldsymbol{A}\boldsymbol{p}_m^{k-1}) \ni \boldsymbol{\sigma}(t_m^k){:}\boldsymbol{E} \quad \text{for} \quad k=1,\ldots,N_m. \tag{3.6}$$

This semi-implicit scheme admits unique solutions and is unconditionally stable. Indeed, by testing (3.6) by $\boldsymbol{p}_m^k-\boldsymbol{p}_m^{k-1}$ and exploiting the convexity of both F_{SA} and $-F_{\text{mag}}$ we get that

$$R|\boldsymbol{p}_m^k-\boldsymbol{p}_m^{k-1}| + F_{\text{SA}}(\boldsymbol{p}_m^k) - F_{\text{mag}}(\boldsymbol{H}(t_m^k)\cdot\boldsymbol{A}\boldsymbol{p}_m^k)$$
$$\leq F_{\text{SA}}(\boldsymbol{p}_m^{k-1}) - F_{\text{mag}}(\boldsymbol{H}(t_m^k)\cdot\boldsymbol{A}\boldsymbol{p}_m^{k-1}) + \boldsymbol{\sigma}(t_m^k){:}\boldsymbol{E}\cdot(\boldsymbol{p}_m^k-\boldsymbol{p}_m^{k-1}).$$

Hence, by summing up for $k = 1, \ldots, i$ $(i \le N_m)$ and summing by parts we deduce

$$F_{\text{SA}}(\boldsymbol{p}_m^i) - F_{\text{mag}}(\boldsymbol{H}(t_m^i) \cdot \boldsymbol{A} \boldsymbol{p}_m^i) - \boldsymbol{\sigma}(t_m^i) : \boldsymbol{E} \cdot \boldsymbol{p}_m^i + \sum_{k=1}^{i} R |\boldsymbol{p}_m^k - \boldsymbol{p}_m^{k-1}|$$

$$\le F_{\text{SA}}(\boldsymbol{p}^0) - F_{\text{mag}}(\boldsymbol{H}(0) \cdot \boldsymbol{A} \boldsymbol{p}^0) - \boldsymbol{\sigma}(0) : \boldsymbol{E} \cdot \boldsymbol{p}^0$$

$$- \sum_{k=1}^{i} (\boldsymbol{\sigma}(t_m^k) - \boldsymbol{\sigma}(t_m^{k-1})) : \boldsymbol{E} \cdot \boldsymbol{p}_m^{k-1} - \sum_{k=1}^{i} \left(F_{\text{mag}}(\boldsymbol{H}(t_m^k) \cdot \boldsymbol{A} \boldsymbol{p}_m^{k-1}) - F_{\text{mag}}(\boldsymbol{H}(t_m^{k-1}) \cdot \boldsymbol{A} \boldsymbol{p}_m^{k-1}) \right).$$

By exploiting $F_{\text{mag}} \in C^{1,1}$, the absolute continuity of $\boldsymbol{\sigma}$ and $\boldsymbol{H}$, and the coercivity of the energy, the above right-hand side can be controlled uniformly with respect to the partition diameter τ_m. Eventually, this ensures that $\dot{\boldsymbol{p}}_m$ is uniformly bounded in L^1.

3.3. Quasi-static evolution

We shall now turn our attention to the full quasi-static evolution problem, i.e., the coupling between the constitutive relation (2.12) with the quasi-static equilibrium problem via (2.6). To this aim, let $\Omega \subset \mathbb{R}^3$ indicate the non-empty, bounded, and open reference configuration of the body and assume its boundary $\partial \Omega$ to be smooth. We impose homogeneous Dirichlet conditions $\boldsymbol{u} = \boldsymbol{0}$ on $\Gamma_{\text{Dir}} \subset \partial \Omega$ such that Γ_{Dir} has positive surface measure and prescribe some surface traction $\boldsymbol{G} \in \mathbb{R}^3$ on the remainder part of the boundary $\Gamma_{\text{tr}} = \partial \Omega \setminus \Gamma_{\text{Dir}}$. Finally, let $\boldsymbol{F} \in \mathbb{R}^3$ be some given body force. The quasi-static equilibrium problem reads

$$\nabla \cdot \boldsymbol{\sigma} + \boldsymbol{F} = \boldsymbol{0} \quad \text{in} \ \ \Omega \times (0, T),$$
$$\boldsymbol{\varepsilon}(\boldsymbol{u}) = \mathbb{C}^{-1} \boldsymbol{\sigma} + \boldsymbol{\varepsilon}_0(\boldsymbol{p}) \quad \text{in} \ \ \Omega \times (0, T),$$
$$\boldsymbol{u} = \boldsymbol{0} \quad \text{in} \ \ \Gamma_{\text{Dir}} \times (0, T), \quad \boldsymbol{\sigma} \boldsymbol{\nu} = \boldsymbol{G} \quad \text{in} \ \ \Gamma_{\text{tr}} \times (0, T)$$

where $\boldsymbol{\nu}$ stands for the outer unit normal to $\partial \Omega$. Let us define

$$\mathcal{U} := \left\{ \boldsymbol{u} \in H^1(\Omega, \mathbb{R}^3) : \boldsymbol{u} = \boldsymbol{0} \text{ on } \Gamma_{\text{Dir}} \right\}, \quad \mathcal{P} := H^1(\Omega; \mathbb{R}^3).$$

and note that we have *Korn's inequality* [76]

$$\|\boldsymbol{u}\|_{\mathcal{U}} \le c_{\text{Korn}} \|\boldsymbol{\varepsilon}(\boldsymbol{u})\|_{L^2(\Omega; \mathbb{R}^{3 \times 3})}$$

for some $c_{\text{Korn}} > 0$ depending only on Ω and Γ_{Dir}. By letting $\boldsymbol{F} : [0, T] \to L^2(\Omega; \mathbb{R}^3)$ and $\boldsymbol{G} : [0, T] \to L^2(\Gamma_{\text{tr}}; \mathbb{R}^3)$, we define the total load $\boldsymbol{\ell} : [0, T] \to \mathcal{U}'$ (dual of $\mathcal{U}$) by

$$\langle \boldsymbol{\ell}(t), \boldsymbol{u} \rangle := \int_{\Omega} \boldsymbol{F} \cdot \boldsymbol{u} \, \mathrm{d}x + \int_{\Gamma_{\text{tr}}} \boldsymbol{G} \cdot \boldsymbol{u} \, \mathrm{d}\Gamma \quad \forall \boldsymbol{u} \in \mathcal{U}, \ t \in [0, T]$$

where $\langle \cdot, \cdot \rangle$ is the duality pairing between $\mathcal{U}'$ and $\mathcal{U}$. Letting $\boldsymbol{H} : [0, T] \to L^1(\Omega; \mathbb{R}^3)$ be given, we define the *total energy functional* $\mathcal{E} : [0, T] \times \mathcal{U} \times \mathcal{P} \longrightarrow (-\infty, \infty]$ by

$$\mathcal{E}(t, \boldsymbol{u}, \boldsymbol{p}) := \frac{1}{2} \int_{\Omega} (\boldsymbol{\varepsilon}(\boldsymbol{u}) - \boldsymbol{\varepsilon}_0(\boldsymbol{p})) : \mathbb{C} : (\boldsymbol{\varepsilon}(\boldsymbol{u}) - \boldsymbol{\varepsilon}_0(\boldsymbol{p})) \, \mathrm{d}x + \int_{\Omega} F_{\text{SA}}(\boldsymbol{p}) \, \mathrm{d}x$$

$$- \int_{\Omega} F_{\text{mag}}(\boldsymbol{H}(t) \cdot \boldsymbol{A} \boldsymbol{p}) \, \mathrm{d}x + \frac{\kappa}{2} \int_{\Omega} |\nabla \boldsymbol{p}|^2 - \langle \boldsymbol{\ell}(t), \boldsymbol{u} \rangle.$$

12

Differently from the constitutive relation case, note that the total energy here contains also an extra *interfacial* term $(\kappa/2)\int_\Omega |\nabla \boldsymbol{p}|^2$ where $\kappa > 0$ is a scale parameter. In particular, the occurrence of such term penalizes phase interfaces and is aimed at reproducing the *finitely twinned* martensitic pattern which is classically observed. From the mathematical viewpoint, the interfacial energy term bears also a crucial compactifying effect.

The dissipation functional $\mathcal{D}: L^1(\Omega; \mathbb{R}^3) \times L^1(\Omega; \mathbb{R}^3) \longrightarrow [0, \infty)$ is defined by

$$\mathcal{D}(\boldsymbol{p}, \boldsymbol{q}) := \int_\Omega D(\boldsymbol{p}-\boldsymbol{q})\,\mathrm{d}x = \int_\Omega R|\boldsymbol{p}-\boldsymbol{q}|\,\mathrm{d}x. \tag{3.7}$$

It is worth pointing out that the dissipation functional $\mathcal{D}$ is continuous with respect to the strong topology of $L^1(\Omega, \mathbb{R}^{3\times 3}) \times L^1(\Omega, \mathbb{R}^{3\times 3})$. Given a suitable initial datum $(\boldsymbol{u}^0, \boldsymbol{p}^0) \in \mathcal{U} \times \mathcal{P}$, we term an *energetic solution of the quasi-static evolution problem* a function $t \in [0, T] \mapsto (\boldsymbol{u}(t), \boldsymbol{p}(t)) \in \mathcal{U} \times \mathcal{P}$ such that $(\boldsymbol{u}(0), \boldsymbol{p}(0)) = (\boldsymbol{u}^0, \boldsymbol{p}^0)$, the function $F'_{\mathrm{mag}}(\boldsymbol{H}\cdot\boldsymbol{Ap})\dot{\boldsymbol{H}}\cdot\boldsymbol{Ap}$ is in $L^1(\Omega\times(0,T))$, and, for every $t \in [0, T]$,

Stability:
$$\mathcal{E}(t, \boldsymbol{u}(t), \boldsymbol{p}(t)) < \infty \quad \text{and} \quad \mathcal{E}(t, \boldsymbol{u}(t), \boldsymbol{p}(t)) \leq \mathcal{E}(t, \widehat{\boldsymbol{u}}, \widehat{\boldsymbol{p}}) + \mathcal{D}(\widehat{\boldsymbol{p}}-\boldsymbol{p}(t)) \quad \forall (\widehat{\boldsymbol{u}}, \widehat{\boldsymbol{p}}) \in \mathcal{U} \times \mathcal{P};$$
$$\tag{3.8}$$

Energy balance:
$$\mathcal{E}(t, \boldsymbol{u}(t), \boldsymbol{p}(t)) + \mathrm{Diss}_{\mathcal{D}}(\boldsymbol{p}, [0, t]) \leq \mathcal{E}(0, \boldsymbol{u}^0, \boldsymbol{p}^0) - \int_0^t \langle \dot{\boldsymbol{\ell}}, \boldsymbol{u} \rangle - \int_0^t \int_\Omega F'_{\mathrm{mag}}(\boldsymbol{H}\cdot\boldsymbol{Ap})\dot{\boldsymbol{H}}\cdot\boldsymbol{Ap}$$
$$\tag{3.9}$$

where $\mathrm{Diss}_{\mathcal{D}}(\boldsymbol{p}, [0, t])$ is constructed exactly as in (3.3) but now starting from the functional $\mathcal{D}$. The existence result reads as follows.

Theorem 3.3 (Existence for quasistatic evolution (Thm. 3.2 [24])). *Let $\boldsymbol{F} \in W^{1,1}(0, T; L^2(\Omega; \mathbb{R}^3))$, $\boldsymbol{G} \in W^{1,1}(0, T; L^2(\Gamma_{\mathrm{tr}}; \mathbb{R}^3))$, $\boldsymbol{H} \in W^{1,1}(0, T; L^1(\Omega; \mathbb{R}^3))$, and $(\boldsymbol{u}^0, \boldsymbol{p}^0)$ be stable, namely fulfilling (3.8) at $t = 0$. Then, there exists an energetic solution of the quasi-static evolution problem.*

Exactly as in the constitutive relation case, this existence result is constructive: one passes to the limit in sequence of time-discretized problems

$$(\boldsymbol{u}_m^0, \boldsymbol{p}_m^0) = (\boldsymbol{u}^0, \boldsymbol{p}^0) \tag{3.10}$$
$$(\boldsymbol{u}_m^k, \boldsymbol{p}_m^k) \in \arg\min \left(\mathcal{E}(t_m^k, \boldsymbol{u}, \boldsymbol{p}) + \mathcal{D}(\boldsymbol{p}-\boldsymbol{p}_m^{k-1}) \right) \tag{3.11}$$

which are solvable as the involved functionals are coercive and lower semicontinuous. The latter minimization problem corresponds to a suitable variational version of the following implicit Euler discretization scheme, for $k = 1, \ldots, N_m$,

$$\nabla\cdot\boldsymbol{\sigma}_m^k + \boldsymbol{F}(t_m^k) = \boldsymbol{0} \quad \text{in} \ \Omega \times (0, T),$$
$$\boldsymbol{\varepsilon}(\boldsymbol{u}_m^k) = \mathbb{C}^{-1}\boldsymbol{\sigma}_m^k + \boldsymbol{\varepsilon}_0(\boldsymbol{p}_m^k) \quad \text{in} \ \Omega \times (0, T),$$
$$\boldsymbol{u}_m^k = \boldsymbol{0} \quad \text{in} \ \Gamma_{\mathrm{Dir}} \times (0, T), \quad \boldsymbol{\sigma}_m^k\boldsymbol{\nu} = \boldsymbol{G}(t_m^k) \quad \text{in} \ \Gamma_{\mathrm{tr}} \times (0, T), \quad \nabla\boldsymbol{p}_m^k\boldsymbol{\nu} = \boldsymbol{0} \quad \text{in} \ \Gamma \times (0, T),$$
$$\partial D(\boldsymbol{p}_m^k-\boldsymbol{p}_m^{k-1}) + \partial F_{\mathrm{SA}}(\boldsymbol{p}_m^k) - \mathrm{D}_{\boldsymbol{p}}F_{\mathrm{mag}}(\boldsymbol{H}(t_m^k)\cdot\boldsymbol{Ap}_m^k) - \kappa\Delta\boldsymbol{p}_m^k \ni \boldsymbol{\sigma}_m^k\!:\!\boldsymbol{E} \quad \text{in} \ \Omega \times (0, T).$$

By denoting again $(\boldsymbol{u}_m, \boldsymbol{p}_m)$ as the right-continuous piecewise constant interpolant the m-th partition of the vector of discrete solutions $\{(\boldsymbol{u}_m^k, \boldsymbol{p}_m^k)\}_{k=0}^{N_m}$, we have the following convergences.

Theorem 3.4 (Convergence of time-discretizations (Cor. 3.3 [24])). *Up to not relabeled subsequences, for all $t \in [0, T]$,*

$$\boldsymbol{p}_m(t) \to \boldsymbol{p}(t) \quad \text{strongly in } \mathcal{P}, \quad \boldsymbol{u}_m(t) \to \boldsymbol{u}(t) \quad \text{strongly in } \mathcal{U},$$
$$\mathcal{E}(t, \boldsymbol{u}_m(t), \boldsymbol{p}_m(t)) \to \mathcal{E}(t, \boldsymbol{u}(t), \boldsymbol{p}(t)), \quad \text{Diss}_{\mathcal{D}}(\boldsymbol{p}_m, [0, t]) \to \text{Diss}_{\mathcal{D}}(\boldsymbol{p}, [0, t])$$

where $(\boldsymbol{u}, \boldsymbol{p})$ is an energetic solution of the quasi-static evolution problem.

We shall comment that the *weak* convergences of $\boldsymbol{p}_m$ and $\boldsymbol{u}_m$ follow directly from classical weak compactness methods whereas the claimed *strong* convergence is consequence of the convergence of the energy as this is uniformly convex up to a continuous perturbation.

Eventually, the quasi-static evolution problem can be controlled by means of the magnetic field $t \mapsto \boldsymbol{H}(t)$. The reader is referred to [49] for some results on existence of optimal controls for a suitably general class of functionals.

3.4. Space approximation

The time-discretization described above can be combined with an approximation in space by conformal finite elements. In particular, we choose nested sequences of finite-dimensional subspaces $\mathcal{U}_j \subset \mathcal{U}$ and $\mathcal{P}_j \subset \mathcal{P}$ such that $\mathcal{U}_j \subset \mathcal{U}_{j+1}$, $\mathcal{P}_j \subset \mathcal{P}_{j+1}$ and the unions $\cup_j \mathcal{U}_j$ and $\cup_j \mathcal{P}_j$ are dense in $\mathcal{U}$ and $\mathcal{P}$, respectively. Suitable finite-dimensional approximation spaces are, for instance, finite-element spaces of continuous piecewise affine functions on a triangulation of the domain (assumed here to be a polyhedron). We shall denote by $\pi_{\mathcal{U}_j} : \mathcal{U} \to \mathcal{U}_j$ and $\pi_{\mathcal{P}_j} : \mathcal{P} \to \mathcal{P}_j$ suitable projections operators (see [29]).

We now define the space-approximated energy and dissipation functionals by restriction, namely

$$\mathcal{E}_j(t, \boldsymbol{u}, \boldsymbol{p}) := \begin{cases} \mathcal{E}(t, \boldsymbol{u}, \boldsymbol{p}) & \text{if } (\boldsymbol{u}, \boldsymbol{p}) \in \mathcal{U}_j \times \mathcal{P}_j, \\ \infty & \text{else,} \end{cases} \qquad \mathcal{D}_j(\boldsymbol{p}, \hat{\boldsymbol{p}}) := \begin{cases} \mathcal{D}(\boldsymbol{p}, \hat{\boldsymbol{p}}) & \text{if } \boldsymbol{p}, \hat{\boldsymbol{p}} \in \mathcal{P}_j, \\ \infty & \text{else.} \end{cases}$$

Let the space-approximated initial datum be $(\boldsymbol{u}_j^0, \boldsymbol{p}_j^0) = (\pi_{\mathcal{U}_j}(\boldsymbol{u}^0), \pi_{\mathcal{P}_j}(\boldsymbol{p}^0))$, assume it to be stable for all j, and that $\mathcal{E}_j(0, \boldsymbol{u}_j^0, \boldsymbol{p}_j^0) \to \mathcal{E}(0, \boldsymbol{u}^0, \boldsymbol{p}^0)$. We consider the sequence $(\boldsymbol{u}_{mj}^k, \boldsymbol{p}_{mj}^k) \in \mathcal{U}_j \times \mathcal{P}_j$ of fully-discrete solutions solving of the incremental minimization problems

$$\min \left(\mathcal{D}_j(\boldsymbol{p} - \boldsymbol{p}_{mj}^{k-1}) + E_j(t_m^k, \boldsymbol{u}, \boldsymbol{p}) \right) = \min_{(\boldsymbol{u}, \boldsymbol{p}) \in \mathcal{U}_j \times \mathcal{P}_j} \left(\mathcal{D}(\boldsymbol{p} - \boldsymbol{p}_{mj}^{k-1}) + E(t_m^k, \boldsymbol{u}, \boldsymbol{p}) \right) \quad \text{for } k = 1, \ldots, N_m,$$

starting from the initial position $(\boldsymbol{u}_{mj}^0, \boldsymbol{p}_{mj}^0) = (\boldsymbol{u}_j^0, \boldsymbol{p}_j^0)$. The existence of such minimizers is ensured by the lower semicontinuity and coercivity of the functionals. In particular, given the specific choice of the finite-dimensional subspaces, the latter minimization problem corresponds to a fully-discrete scheme. We denote the right-continuous interpolants on the time-partitions of the fully-discrete solutions by $(\boldsymbol{u}_{mj}, \boldsymbol{p}_{mj})$. By applying the general Γ-convergence theory from [68] one can deduce convergence of $(\boldsymbol{u}_{mj}, \boldsymbol{p}_{mj})$.

14

Theorem 3.5 (Convergence of space-time discretizations (Thm. 3.4 [68])). *Up to not relabeled subsequences we have that, for all $t \in [0, T]$,*

$$\boldsymbol{p}_{mj}(t) \to \boldsymbol{p}(t) \quad strongly\ in\ \ \mathcal{P}, \quad \boldsymbol{u}_{mj}(t) \to \boldsymbol{u}(t) \quad strongly\ in\ \ \mathcal{U},$$

$$\mathcal{E}_j(t, \boldsymbol{u}_{mj}(t), \boldsymbol{p}_{mj}(t)) \to \mathcal{E}(t, \boldsymbol{u}(t), \boldsymbol{p}(t)), \quad \mathrm{Diss}_{\mathcal{D}_j}(\boldsymbol{p}_{mj}, [0, t]) \to \mathrm{Diss}_{\mathcal{D}}(\boldsymbol{p}, [0, t])$$

where $(\boldsymbol{u}, \boldsymbol{p})$ is an energetic solution of the quasi-static evolution problem.

The reader is referred to [29] and [46, 47] for some analogous convergence statements, although in the non-magnetic case. In particular, the analysis in [46] suggests that, even for the present magnetomechanical coupling situation, we would be in the position of proving suitable a priori error estimates for fully discretized solutions.

4. Implementation and numerical testing

In this section, we introduce a numerical algorithm to solve the zero-dimensional constitutive problem in a 3D setting (or, equivalently, to solve the constitutive problem at the Gauss point level within a finite element discretization of a 3D body). We then numerically test the behavior of the constitutive model under a varying magnetic field and a constant uniaxial stress.

4.1. Time discretization and solution algorithm

Let us now focus on the crucial issue of numerically solving at the Gauss point level the set of constitutive equations described in Section 2.5, considering the flow rule of Section 2.6 and taking advantage of the reduced formulation of Section 2.7. We shall directly concentrate ourselves on the solution of the time-incremental problem. Namely, we discretize the time-interval of interest $[0, T]$ by means of the partition $\{0 = t_0 < t_1 < ... < t_{N-1} < t_n = T\}$, assume to be given the state of the system $(\boldsymbol{\varepsilon}_n, \boldsymbol{\varepsilon}_{0,n}, \boldsymbol{p}_n)$ at time t_n, the driving fields $(\boldsymbol{\sigma}_{n+1}, \boldsymbol{H}_{n+1})$ and temperature T_{n+1} at time t_{n+1}, and solve for $(\boldsymbol{\varepsilon}_{n+1}, \boldsymbol{\varepsilon}_{0,n+1}, \boldsymbol{p}_{n+1})$. For the sake of numerical convenience, we perform some regularization on the term $\beta^*|\boldsymbol{\varepsilon}_0(\boldsymbol{p})|$; in particular, in such a term, we substitute the standard Euclidean norm with its regularized version $\overline{|\cdot|}$, defined as

$$\overline{|\boldsymbol{a}|} = \sqrt{|\boldsymbol{a}|^2 + \epsilon} - \sqrt{\epsilon},$$

where ϵ is a user-defined parameter controlling the smoothness of the norm regularization, typically selected to be very small (e.g., 10^{-8}).

The flow rule is time-integrated following a standard backward-Euler method and the model is completed by the discrete complementary conditions:

$$\Delta\zeta \geq 0, \quad F \leq 0, \quad \Delta\zeta F = 0, \tag{4.12}$$

where $\Delta\zeta = \zeta - \zeta_n = \int_{t_n}^{t_{n+1}} \dot{\zeta}dt$ is the time-integrated consistency parameter.

The solution of the discrete model is performed by means of an elastic-predictor inelastic-corrector return map procedure as in classical plasticity problems (the interested reader is referred to [77, 31] for a complete discussion on algorithmic details). An elastic trial state is

evaluated keeping frozen the internal variables, then a trial value of the limit function is computed to verify the admissibility of the trial state. If this is not verified, the step is inelastic and the evolution equations have to be integrated.

We remark that, as in [31], we distinguish two inelastic phases in our model: a non-saturated phase and a saturated one. In our solution procedure we start assuming to be in a non-saturated phase, and when convergence is attained we check if our assumption is violated. If the non-saturated solution is not admissible, we search for a new solution considering saturated conditions.

Eventually, we highlight that in this solution algorithm we implement the semi-implicit scheme discussed in Section 3.2.

4.2. Numerical testing

We finally perform a numerical experiment in order to test the behavior of the model and assess its capability to reproduce the typical response of magnetic shape memory alloys under a varying magnetic field and a constant uniaxial stress.

With this aim, we consider a zero-dimensional constitutive problem in a 3D setting characterized by the material parameters reported in Table 4.2. We apply a cyclic magnetic field between $\pm 6 \cdot 10^5$ A m^{-1} acting along the $\boldsymbol{e}^2$-direction, under different values of constant compressive stress acting in the $\boldsymbol{e}^1$-direction. The system of nonlinear equations arising from the discrete problem as described above is then numerically solved by means of the function *fsolve* implemented in the optimization toolbox of the program MATLAB®.

parameter	value	unit
E	$800 \cdot 10^6$	Pa
ν	0.3	-
β^*	0	Pa
h	$790 \cdot 10^4$	Pa
R	10^5	Pa
ε_L	0.062	-
m_{sat}	$514 \cdot 10^3$	A m^{-1}
μ_0	$4\pi \cdot 10^{-7}$	N A^{-2}
δ	1	Pa^{-1}
ϵ	10^{-8}	-

Table 1: Material parameters.

The obtained results are reported in Figure 1, where, for the different considered levels of the compressive stress (σ_{11}), we plot the relevant component of the transformation strain ($\varepsilon_{0,11} = \boldsymbol{\varepsilon}_0(\boldsymbol{p})_{11}$) as a function of the $\boldsymbol{e}^2$-component of the magnetic field (H_2). In particular, it is important to observe that the typical cyclic behavior of magnetic shape memory alloys (cf., e.g., [17]) is correctly reproduced by the proposed model, which is able to capture also the blocking stress effect (cf. Section 2.11).
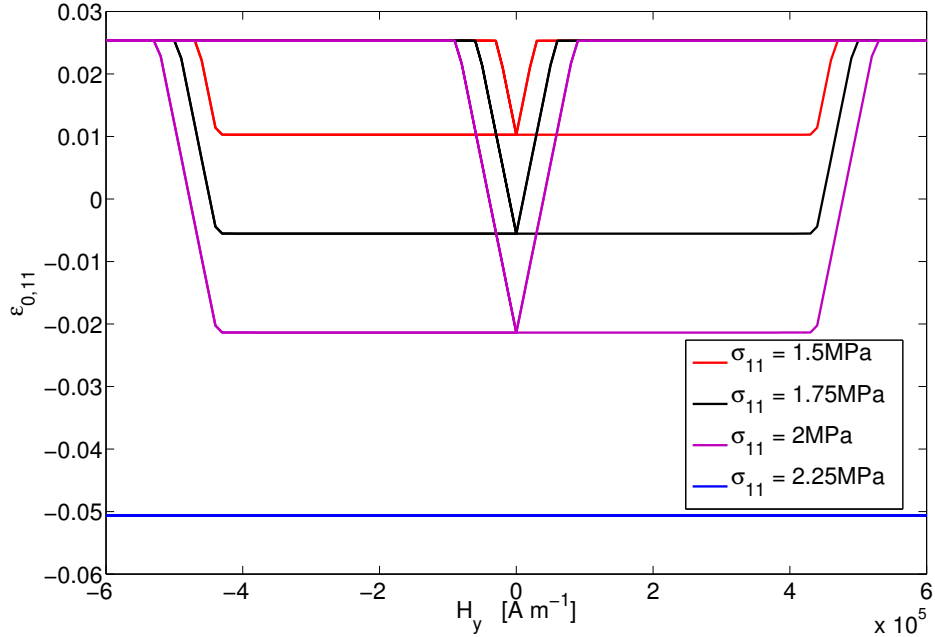
Figure 1: Magnetically-induced transformation strain under constant compression: transformation strain versus magnetic field, for different compression levels.

5. Conclusions

In this paper, a three-dimensional phenomenological model describing the magneto-mechanical behavior of magnetic shape-memory alloys has been introduced. A thermodynamically-consistent constitutive relation has been proposed moving from micromagnetic considerations. Such a model has been shown to be capable of reproducing the magnetically-induced martensitic transformation in single crystals, including important effects such as the so-called *blocking-stress*. Existence results for the constitutive relation problem as well as for the corresponding quasi-static evolution system have been illustrated, along with the convergence of time- and space-time-discretizations. Algorithmic considerations have also been presented and the model has been numerically tested, confirming its capability to reproduce the typical response of magnetic shape-memory alloys.

17

References

[1] Frémond M, 1987. Matériaux à mémoire de forme. *C. R. Acad. Sci. Paris Sér. II Méc. Phys. Chim. Sci. Univers Sci. Terre*, 304: 239–244.

[2] Duerig TW, Pelton AR editors, 2003. *SMST-2003 Proceedings of the International Conference on Shape Memory and Superelastic Technology Conference*. ASM International.

[3] Roubíček T, 2004. Models of microstructure evolution in shape memory alloys. In *Nonlinear Homogenization and its Appl.to Composites, Polycrystals and Smart Materials*, P. Ponte Castaneda, J. J. Telega, B. Gambin eds., NATO Sci. Series II/170, Kluwer, Dordrecht, 269–304.

[4] Auricchio F, Sacco E, 1997. A one-dimensional model for superelastic shape-memory alloys with different elastic properties between austenite and martensite. *Int. J. Non-Linear Mech.*, 32: 1101–1114.

[5] Falk F, Konopka P, 1990. Three-dimensional Landau theory describing the martensitic phase transformation of shape-memory alloys. *J. Phys. Condens. Matter*, 2: 61–77.

[6] Govindjee S, Miehe C, 2001. A multi-variant martensitic phase transformation model: formulation and numerical implementation. *Comput. Methods Appl. Mech. Engrg.*, 191: 215–238.

[7] Helm D, Haupt P, 2003: Shape memory behaviour: modelling within continuum thermomechanics. *Internat. J. Solids Structures*, 40: 827–849.

[8] Lagoudas DC, Entchev PB, Popov P, Patoor E, Brinson LC, Gao X, 2006. Shape memory alloys, Part II: Modeling of polycrystals. *Mech. Materials*, 38: 391–429.

[9] Levitas VI, 1998. Thermomechanical theory of martensitic phase transformations in inelastic materials. *Internat. J. Solids Structures*, 35: 889–940.

[10] Peultier B, Ben Zineb T, Patoor E, 2006. Macroscopic constitutive law for SMA: Application to structure analysis by FEM. *Materials Sci. Engrg. A*, 438–440: 454–458.

[11] Popov P, Lagoudas DC, 2007. A 3-D constitutive model for shape memory alloys incorporating pseudoelasticity and detwinning of self-accommodated martensite. *Internat. J. Plast.*, 23: 1679–1720.

[12] Raniecki B, Lexcellent C, 1994. R_L models of pseudoelasticity and their specification for some shape-memory solids. *Eur. J. Mech. A Solids*, 13: 21–50.

[13] Reese S, Christ D, 2008. Finite deformation pseudo-elasticity of shape memory alloys – Constitutive modelling and finite element implementation. *Internat. J. Plast.*, 28: 455–482.

[14] Thamburaja P, Anand L. 2001. Polycrystalline shape-memory materials: effect of crystallographic texture. *J. Mech. Phys. Solids*, 49: 709-737.

[15] DeSimone A, James RD, 2002. A constrained theory of magnetoelasticity. *J. Mech. Phys. Solids*, 50: 283–320.

[16] James RD, Wuttig M, 1998. Magnetostriction of martensite. *Phil. Mag. A,* 77: 1273-1299.

[17] Karaca HE, Karaman I, Basaran B, Chumlyakov YI, Maier HJ, 2006. Magnetic field and stress induced martensite reorientation in NiMnGa ferromagnetic shape memory alloy single crystals. *Acta Mat.*, 54: 233–245.

[18] Likhachev AA, Ullakko K, 2000. Magnetic-field-controlled twin boundaries motion and giant magneto-mechanical effects in NiMnGa shape memory alloy. *Phys. Lett. A*, 275: 142–151.

[19] O'Handley RC, 1998. Model for strain and magnetization in magnetic shape-memory alloys, *J. Appl. Phys.*, 83: 3263–3270.

[20] Tickle R, James RD, 1999. Magnetic and magnetomechanical properties of Ni_2MnGa. *J. Magn. Magn. Mater.*, 195: 627–638.

[21] Kiang J, Tong L, 2005. Modelling of magneto-mechanical behaviour of NiMnGa single crystals. *J. Magn. Magn. Mater.*, 292: 394–412.

[22] Auricchio, Bessoud A-L, Reali A, Stefanelli U, 2010. Macroscopic modeling of magnetic shape memory alloys. *Oberwolfach Reports*, 14/2010: 771–773.

[23] Auricchio, Bessoud A-L, Reali A, Stefanelli U, 2011. A three-dimensional phenomenological model for Magnetic Shape Memory Alloys. *GAMM-Mitt.*, 34: 90–96.

[24] Bessoud A-L, Stefanelli U, 2011. Magnetic Shape Memory Alloys: three-dimensional modeling and analysis. *Math. Models Met. Appl. Sci.*, 21: 1043–1069.

[25] Auricchio F, Petrini L, 2002. Improvements and algorithmical considerations on a recent three-dimensional model describing stress-induced solid phase transformations. *Internat. J. Numer. Methods Engrg.*, 55: 1255–1284.

[26] Auricchio F, Petrini L, 2004. A three-dimensional model describing stress-temperature induced solid phase transformations. Part I: solution algorithm and boundary value problems. *Internat. J. Numer. Methods Engrg.*, 61: 807–836.

[27] Auricchio F, Petrini L, 2004. A three-dimensional model describing stress-temperature induced solid phase transformations. Part II: thermomechanical coupling and hybrid composite applications. *Internat. J. Numer. Methods Engrg.*, 61: 716–737.

[28] Souza AC, Mamiya EN, Zouain N, 1998. Three-dimensional model for solids undergoing stress-induces transformations. *Eur. J. Mech. A Solids*, 17: 789-806.

[29] Auricchio F, Mielke A, Stefanelli U, 2008. A rate independent model for the isothermal quasi-static evolution of shape-memory materials. *Math. Models Methods Appl. Sci.*, 18: 125–164.

[30] Auricchio, Reali A, Stefanelli U, 2009. A macroscopic 1D model for shape memory alloys including asymmetric behaviors and transformation-dependent elastic properties. *Comput. Methods Appl. Mech. Engrg.*, 198: 1631–1637.

[31] Auricchio, Reali A, Stefanelli U, 2007. A three-dimensional model describing stress-induced solid phase transformation with permanent inelasticity. *Internat. J. Plast.*, 23: 207–226.

19

[32] Auricchio, Reali A, Stefanelli U, 2007. A phenomenological 3D model describing stress-induced solid phase transformations with permanent inelasticity. In *Topics on Mathematics for Smart Systems*, 1–14, World Sci. Publishing.

[33] Eleuteri M, Lussardi L, Stefanelli U, 2011. A rate-independent model for permanent inelastic effects in shape memory materials. *Netw. Heterog. Media*, 6:145–165.

[34] Arghavani J, Auricchio F, Naghdabadi R, Reali A, 2011. On the robustness and efficiency of integration algorithms for a 3D finite strain phenomenological SMA constitutive model. *Internat. J. Numer. Methods Engrg.*, 85: 107–134.

[35] Arghavani J, Auricchio A, Naghdabadi R, Reali A, 2011. An improved, fully symmetric, finite strain phenomenological constitutive model for shape memory alloys. *Fin. Elem. in Anal. and Des.*, 47: 166–174.

[36] Arghavani J, Auricchio F, Naghdabadi R, Reali A, Sohrabpour S, 2010. A 3D finite strain phenomenological constitutive model for shape memory alloys considering martensite reorientation. *Contin. Mech. Thermodyn.*, 22: 345–362.

[37] Evangelista V, Marfia S, Sacco E, 2009. Phenomenological 3D and 1D consistent models for shape-memory alloy materials. *Comput. Mech.*, 44: 405–421.

[38] Evangelista V, Marfia S, Sacco E, 2010. A 3D SMA constitutive model in the framework of finite strain. *Internat. J. Numer. Methods Engrg.*, 81: 761–785.

[39] Frigeri S, Stefanelli U, 2012. Existence and time-discretization for the finite-strain Souza-Auricchio constitutive model for shape-memory alloys. *Contin. Mech. Thermodyn.*, 24: 63–77.

[40] Mielke A, Paoli L, Petrov A, 2009. On existence and approximation for a 3D model of thermally-induced phase transformations in shape-memory alloys. *SIAM J. Math. Anal.*, 41: 1388–1414.

[41] Mielke A, Petrov A, 2007. Thermally driven phase transformation in shape-memory alloys. *Adv. Math. Sci. Appl.*, 17: 667–685.

[42] Krejčí P, Stefanelli U, 2010. Well-posedness of a thermo-mechanical model for shape memory alloys under tension. *M2AN Math. Model. Anal. Numer.*, 44:1239–1253.

[43] Krejčí P, Stefanelli U, 2011. Existence and nonexistence for the full thermomechanical Souza-Auricchio model of shape memory wires, *Math. Mech. Solids*, 16:349–365.

[44] Paoli L, Petrov A, 2011. Global existence result for phase transformations with heat transfer in shape memory alloys. Preprint arXiv:1104.5408.

[45] Roubíček T, Stefanelli U, 2013. Thermomechanics of magnetic shape-memory crystals: modeling and analysis. In preparation.

[46] Mielke A, Paoli L, Petrov A, Stefanelli U, 2010. Error estimates for discretizations of a rate-independent variational inequality. *SIAM J. Numer. Anal.*, 48: 1625–1646.

[47] Mielke A, Paoli L, Petrov A, Stefanelli U, 2009. Error bounds for space-time discretizations of a 3D model for shape-memory alloys. In the Proceedings of the *IUTAM Symposium on Variational Concepts with Applications to the Mechanics of Materials*. IUTAM Bookseries, Springer.

[48] Eleuteri M, Lussardi L, Stefanelli U, 2013. Thermal control of the Souza-Auricchio model for shape memory alloys. *Discrete Cont. Dyn. Syst.-S*, 6: 369–386.

[49] Stefanelli U, 2012. Magnetic control of magnetic shape-memory single crystals. *Phys. B*, 407: 1316–1321.

[50] Bessoud A-L, Kružík M, Stefanelli U, 2012. A macroscopic model for magnetic shape memory alloys. *Z. Angew. Math. Phys.*, to appear.

[51] Murray SJ, Allen SM, O'Handley RC, Lograsso TA, 2000. Magnetomechanical performance and mechanical properties of Ni-Mn-Ga ferromagnetic shape memory alloys. In: *SPIE Proceedings*, 3992: 387.

[52] Murray SJ, O'Handley RC, Allen SM, 2000. Model for discontinuous actuation of ferromagnetic shape memory alloy under stress. *J. Appl. Phys.* 89: 1295–1301.

[53] Tickle R, James RD, Shield T, Wuttig M, Kokorin VV, 1999. Ferromagnetic shape memory in the NiMnGa system. *IEEE Trans. Mag.*, 35: 4301–4310.

[54] Murray SJ, Marioni M, Tello PG, Allen SM, O'Handley RC, 2001. Giant magnetic-field-induced strain in Ni-Mn-Ga crystals: experimental results and modeling. *J. Magn. Magn. Mater.*, 226–230: 945–947.

[55] O'Handley RC, Murray SJ, Marioni M, Nembach H, Allen SM, 2000. Phenomenology of giant magnetic-field-induced strain in ferromagnetic shape-memory materials. *J. Appl. Phys.*, 87:4712–4717.

[56] Adly A, Davino D, Visone C, 2006. Simulation of field effects on the mechanical hysteresis of terfenol rods and magnetic shape memory materials using vector Preisach-type models. *Phys. B*, 372: 207–210.

[57] Hirsinger L, Lexcellent C, 2003. Internal variable model for magneto-mechanical behaviour of ferromagnetic shape memory alloys Ni-Mn-Ga. *J. Phys. IV*, 112: 977–980.

[58] Hirsinger L, 2004. Ni-Mn-Ga shape memory alloys: modelling of magneto-mechanical behaviour. *Int. J. Appl. Electromagn. Mech.*, 19: 473–477.

[59] Gauthier J-Y, Lexcellent C, Hubert A, Abadie J, Chaillet N, 2011. Magneto-thermo-mechanical modeling of a magnetic shape memory alloy Ni-Mn-Ga single crystal. *Ann. Solid Struct. Mech.*, 2: 19–31.

[60] Kiefer B, 2006. A phenomelogical model for magnetic sape memory alloys. PhD Thesis, Texas A&M.

[61] Kiefer B, Lagoudas DC, 2009. Modeling the coupled strain and magnetization response of magnetic shape memory alloys under magnetomechanical loading. *J. Intell. Mater. Syst. Struct.*, 20: 143–170.

[62] Kiefer B, Karaca H, Lagoudas DC, Karaman I, 2007. Characterization and modeling of the magnetic field-induced strain and work output in Ni_2MnGa magnetic shape memory alloys. *J. Magn. Magn. Mater.*, 312: 164–175.

[63] Miehe C, Kiefer B, Rosato D, 2011. An incremental variational formulation of dissipative magnetostriction at the macroscopic continuum level. *Internat. J. Solids Struct.*, 48: 1846–1866.

[64] Wang J, Steinmann P, 2012. A variational approach towards the modelling of magnetic field-induced strains in magnetic shape memory alloys. *J. Mech. Phys. Solids*, 60:1179–1200.

[65] Chen X, Moumni Z, He Y, Xhang W, 2014. A three-dimensional model of magneti-mechanical behaviors of martensite reorientation in ferromagnetic shape memory alloys. *J. Mech. Phys. Solids*, 64:249–286.

[66] Zhu Y, Dui G, 2007. Micromechanical modeling of the stress-induced superelastic strain in magnetic shape memory alloy. *Mech. Materials*, 39: 1025-1034.

[67] Zhu Y, Dui G, 2008. Model for field-induced reorientation strain in magnetic shape memory alloys with tensile and compressive loads. *J. Alloys Compd.*, 459: 55–60.

[68] Mielke A, Roubíček T, Stefanelli U, 2008. Γ-limits and relaxations for rate-independent evolutionary problems. *Calc. Var. Partial Differential Equations*, 31: 387–416.

[69] Mielke A, 2005. Evolution in rate-independent systems (ch. 6). In C. Dafermos and E. Feireisl editors. *Handbook of Differential Equations, Evolutionary Equations*, vol. 2, 461-559. Elsevier B.V.

[70] Conti S, Lenz M, Rumpf M, 2008. Macroscopic behaviour of magnetic shape-memory poly-crystals and polymer composites. *Mater. Sci. Engrg. A*, 481-482: 351–355.

[71] Sozinov A, Likhachev AA, Lanska N, Ullakko K, 2002. Giant magnetic-field-induced strain in NiMnGa seven-layered martensitic phase. *Appl. Phys. Lett.*, 80: 1746–1748.

[72] Brézis H, 1973. *Operateurs maximaux monotones et semi-groupes de contractions dans les espaces de Hilbert*, Math Studies, Vol.5, North-Holland, Amsterdam/New York.

[73] Cullity BD, Graham CD, 2008. *Introduction to magnetic materials*. Second ed., Wiley.

[74] Bhattacharya K, 2003. *Microstructures of Martensites*. Oxford Series on Materials Modeling, Oxford University Press, Oxford.

[75] Mielke A, Theil F, 2004. On rate-independent hysteresis models. *NoDEA Nonlinear Diff. Equations Applications*, 11: 151–189.

[76] Duvaut G, Lions J-L, 1976. *Inequalities in Mechanics and Physics*. Springer.

[77] Arghavani J, Auricchio F, Naghdabadi R, Reali A, Sohrabpour S, 2010. A 3-D phenomeno-logical model for shape memory alloys under multiaxial loadings. *Internat. J. Plast.*, 26:976–991.